

CONFINEMENT AND LIGHT-FRONT QCD <sup>a</sup>

M. BURKARDT

Department of Physics, New Mexico State University  
Las Cruces, New Mexico 88003-0001 USA

## Abstract

Numerical results for the (rest-frame)  $Q\bar{Q}$  potential in light-front quantized  $QCD_{2+1}$  on a  $\perp$  lattice are presented. Both in the longitudinal as well as the  $\perp$  spatial directions one obtains linear confinement. The confinement mechanism in light-front QCD depends on the orientation of the external charges: for longitudinally (with respect to the boost direction in the infinite momentum frame) separated quarks, confinement arises from the instantaneous interaction piece in the Hamiltonian while for  $\perp$  separated quarks, the confinement mechanism is similar to the one in Hamiltonian lattice QCD. Nevertheless, already a very simple ansatz for the effective link-field potential yields an almost rotationally symmetric  $Q\bar{Q}$  potential. The momentum carried by the glue strongly depends on the orientation ("polarization") of the  $Q\bar{Q}$  pair.

Light-front (LF) quantization is the most physical approach to calculating parton distributions on the basis of QCD<sup>1</sup>. In the transverse lattice formulation of QCD<sup>2</sup>, one keeps the time direction and one spatial direction continuous and discretizes the transverse spatial directions. The space time geometry is thus an array of  $1 + 1$  dimensional sheets (Fig. 1). One the one hand, this provide both UV and IV cutoffs in the transverse directions and on the other hand one can still perform LF quantization since the longitudinal directions are continuous. Furthermore, in the compact formulation, it is straightforward to implement Gauss' law as a constraint on the states — avoiding troublesome divergences for  $k^+ \rightarrow 0$ , which plague many other formulations of LF QCD.

Another advantage of the transverse lattice is that confinement is manifest in the limit of large  $\perp$  lattice spacing  $a_\perp$ . The mechanism differs for the longitudinal and the  $\perp$  directions: if one separates a  $Q\bar{Q}$  pair longitudinally then, since  $a_\perp$  is large, the fields in different sheets couple only weakly and the quarks interact only with fields in the same sheet, i.e. effectively the theory reduces to  $1 + 1$  dimensional QCD, where confinement is known to be linear. In contrast, when one separates the  $Q\bar{Q}$  pair transversely, gauge invariance demands that they are connected by a chain of (gluon) link fields. For large  $a_\perp$ , where there are only little fluctuations, this implies that the energy of such a configuration is given by the energy for creating one link quantum times the number of link quanta, i.e. linear confinement also in the  $\perp$  direction. Since the confinement mechanisms are very different for these two cases, one might ask whether a rotationally invariant  $Q\bar{Q}$  potential results in the continuum limit. In fact, in the limit of large  $a_\perp$  one finds in  $2 + 1$  dimensions<sup>3</sup>:

$V(x_L, x_\perp) = \sigma(|x_L| + |x_\perp|)$ , where  $\sigma$  is the string tension, which is clearly not rotationally invariant. In order to investigate this issue, I used DLCQ and a Lanzcos algorithm to calculate the rest frame  $Q\bar{Q}$  potential from the LF Hamiltonian for  $QCD_{2+1}$  on a  $\perp$  lattice. The procedure for computing the rest frame potential in this formalism follows Ref. <sup>5</sup>.

The light-front Hamiltonian for compact QCD on a transverse lattice has been introduced by Bardeen<sup>2</sup>. For pure glue QCD in  $2+1$  dimensions one finds

$$P^- = c_g \sum_n \int dx^- \int dy^- : \text{tr} [J_n(x^-) |x^- - y^-| J_n(y^-)] : + V_{eff}(U), \quad (1)$$

where

$$J_n = U_n^\dagger \overset{\leftrightarrow}{\partial} U_n - U_{n+1}^\dagger \overset{\leftrightarrow}{\partial} U_{n+1} \quad (2)$$

and  $U_n$  are the link fields, which are quantized matrix fields and satisfy the usual commutation relations. Ideally, one would like to work with  $U_n \in SU(N)$ , but in practice this is very complicated<sup>6</sup> and it is advantageous to work with an unconstrained complex matrix field and instead add an

<sup>a</sup>Talk given at 3<sup>rd</sup> AUP workshop on "Confinement, Chaos and Collision", Paris, France, June 96

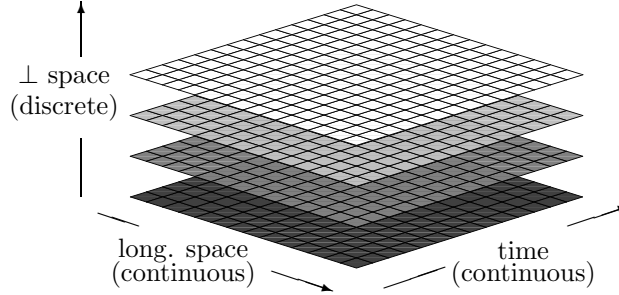


Figure 1: Space time view of a transverse lattice

effective constraint term  $V_{eff}(U)$  to the light-front Hamiltonian. In the case of  $N \rightarrow \infty$ , in the classical limit,  $V_{eff}(U)$  can be taken of the form

$$V_{eff}^{cl}(U) = c_2 \sum_n \text{tr} : [U_n^\dagger U_n] : + c_4 \sum_n \text{tr} : [U_n^\dagger U_n U_n^\dagger U_n] :, \quad (3)$$

where  $c_2 = -2c_4$  and  $c_4 \rightarrow \infty$ , which provides an effective potential which is minimized for  $U_n \in U(N)$ . In the  $N \rightarrow \infty$  limit, the difference between  $U(N)$  and  $SU(N)$  is irrelevant and Eq.(3) is thus suitable for enforcing the  $SU(N)$  constraint in the classical limit. One might be tempted to try a similar ansatz for the LF quantized case. There are several reasons why a different form for the effective potential might be desirable. First, if one would still attempt to work with an effective potential of the above form then physical states would necessarily look extremely complicated, which has to do with the fact that the above ansatz for the effective potential corresponds to working close to the continuum limit. Thus even if the ansatz in Eq.(3) would work in principle, it would most likely not be very practical. Furthermore, since a "mexican hat" potential corresponds to a situation where one is working with the *false* vacuum, it is questionable whether a physical situation where a particle runs at the bottom of a mexican hat can be described at all by a LF Hamiltonian using degrees of freedom expanded around the origin.

For these two reasons, it makes more sense not to consider  $U_n$  as the *bare* link field, but instead think of it as some kind of *blocked* or *smeared* variable. The blocking has several consequences. First, the  $SU(N)$  constraint gets relaxed which reflects itself in the fact that the effective potential is no longer just a narrow valley<sup>7</sup>. Secondly, using smeared variables, it might be easier to cover large physical distances with only few degrees of freedom. The price one has to pay for these advantages is that the effective potential gets more complex and in general more terms are necessary than shown in Eq.(3). In Ref.<sup>8</sup> an attempt has been made to fit the effective potential to the glueball spectrum by making an ansatz which includes all operators up to dimension four. Since this work is a first study of the rest-frame  $Q\bar{Q}$  potential and, as we will discuss below, the  $Q\bar{Q}$  potential turns out to be rather insensitive to terms of dimension greater than two in  $V_{eff}(U)$ , we will instead only consider a much simpler ansatz in the following and keep only the quadratic term

$$V_{eff}(U) \approx c_2 \text{tr} (U^\dagger U). \quad (4)$$

An approximation, where one allows at most one link field quantum per link, was used. Within this approximation, one obtains only a first order phase transition at the critical point, i.e. the lattice spacing always remains finite in physical units. The calculations were done at the critical point, where  $a_\perp \approx 1.04\sigma^{-1/2}$  ( $a_\perp \approx 1.14\sigma^{-1/2}$ ) — with (without) Fock space truncation. The resulting  $Q\bar{Q}$  potential is shown in Fig. 2 as a function of  $r = \sqrt{x_\perp^2 + x_L^2}$ . One free dimensionless parameter was

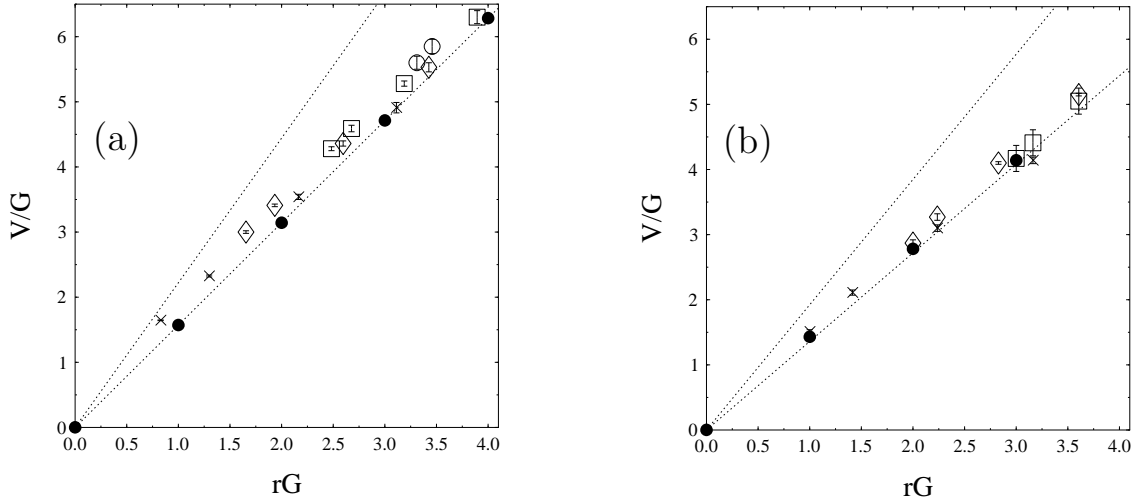


Figure 2: Numerical results for the rest-frame  $Q\bar{Q}$  potential calculated on a  $\perp$  lattice, both with (a) and without (b) Fock space truncation. The various symbols correspond to numerical results obtained from various directions. All dimensionful quantities are in units of the longitudinal coupling  $G$ . The dotted lines are extreme cases in the strong coupling limit. The error bars reflect uncertainties in the continuum extrapolation of the DLCQ results.

adjusted in the calculation to get equal string tensions in the longitudinal and transverse directions (note that this parameter does not affect the numerical calculation but is only relevant for scale setting). For large  $a_\perp$ ,  $V(x_\perp, x_L)$  fills the area between the dotted lines. The symbols are numerical results at the critical point for various directions. The small residual anisotropy is probably due to the use of an oversimplified effective potential. Note that while QED and QCD are equivalent as long as one restricts oneself to only one quantum per link (Fig. 2a), this is no longer the case for the calculations without such a restriction (Fig. 2b).

Intuitively, one would expect a much stronger violation of rotational symmetry than in Fig. 2. The reason this did not happen is probably the following: typically, ground states of LF Hamiltonians are dominated by the lowest Fock component. For the string connecting a  $Q\bar{Q}$  pair, this implies that the wavefunction is dominated by components with only one quantum per link — where higher order terms in the effective potential do not matter. We are currently investigating excited states of the  $Q\bar{Q}$  string, which correspond to hybrid states of quarkonium<sup>3</sup>. In these excited states, higher order terms in the effective potential do matter and we expect to obtain information about the connection between the form of the effective potential and rotational symmetry.

Another physical observable for the  $Q\bar{Q}$  states is the momentum carried by the glue (Fig. 3). One finds a strong anisotropy in the sense that the gluons (link fields) carry much more momentum when the  $Q\bar{Q}$  pair is separated transversely than when it is separated longitudinally (at the same physical distance, i.e. even though the same amount of energy is stored in the gluon field in both cases). Such a result is physical and is familiar from QED<sup>9</sup>. It can be most easily understood from the point-of-view of an infinite momentum boost: if the electric field lines before the boost are  $\perp$  to the boost directions, the field after the boost will look almost like a transverse electromagnetic wave and carries a large (Pointing) momentum. This is not the case when the electric field is parallel to the boost direction. The anisotropy effect is more pronounced in QCD than in QED because the (rest frame) electric field is squeezed into flux tubes. This effect might have measurable consequences in the decays of polarized hybrid states and shows that the difference between confinement mechanisms in LF-QCD for longitudinal and  $\perp$  directions has physical consequences.

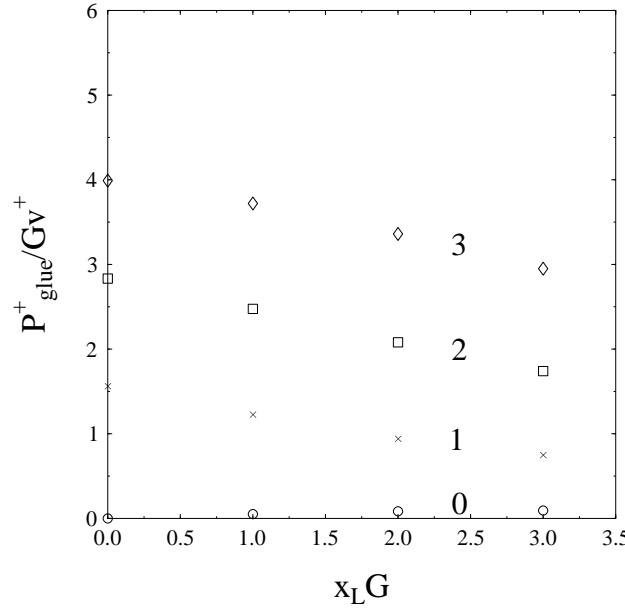


Figure 3: Momentum carried by the gluons for external charges that are separated by  $n_{\perp} = 0, \dots, 3$  lattice spacings as a function of the longitudinal (rest-frame) separation of the external charges. Only the results with inclusion of higher Fock components are shown.

## References

1. M. Burkardt, *Advances Nucl. Phys.* **23**, 1 (1996).
2. W. A. Bardeen et al., *Phys. Rev. D* **21**, 1037 (1980).
3. M. Burkardt and B. Klindworth, submitted to PRD, hep-ph/9601289.
4. M. Burkardt, ELFE Meeting 1995, hep-ph/9510264.
5. M. Burkardt, LF-workshop, Zakopane, Aug 1994, hep-ph/9410219.
6. P. A. Griffin, LF-workshop, Zakopane, Aug 1994, hep-ph/9410243.
7. B. Grossmann et al., *Int. J. Mod. Phys. A* **6**, 2649 (1991).
8. B. vande Sande and S. Dalley, hep-ph/9602291.
9. M. Burkardt, *Nucl. Phys.* **B373**, 613 (1992).